JACS
JOURNAL OF THE AMERICAN CHEMICAL SOCIETY

Subscriber access provided by American Chemical Society

Article

Design, Synthesis, Linear, and Nonlinear Optical Properties of Conjugated (Porphinato)zinc(II)-Based Donor–Acceptor Chromophores Featuring Nitrothiophenyl and Nitrooligothiophenyl Electron-Accepting Moieties

Tian-Gao Zhang, Yuxia Zhao, Inge Asselberghs, Andr Persoons, Koen Clays, and Michael J. Therien

J. Am. Chem. Soc., **2005**, 127 (27), 9710-9720• DOI: 10.1021/ja0402553 • Publication Date (Web): 17 June 2005

Downloaded from http://pubs.acs.org on March 25, 2009

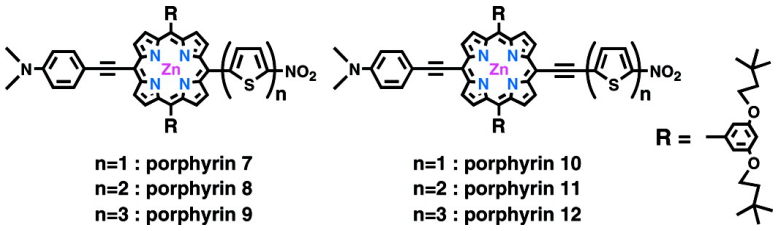

n=1 : porphyrin 7
n=2 : porphyrin 8
n=3 : porphyrin 9

n=1 : porphyrin 10
n=2 : porphyrin 11
n=3 : porphyrin 12

More About This Article

Additional resources and features associated with this article are available within the HTML version:

- Supporting Information
- Links to the 20 articles that cite this article, as of the time of this article download
- Access to high resolution figures
- Links to articles and content related to this article
- Copyright permission to reproduce figures and/or text from this article

View the Full Text HTML

ACS Publications
High quality. High impact.

Journal of the American Chemical Society is published by the American Chemical Society. 1155 Sixteenth Street N.W., Washington, DC 20036

J|A|C|S
ARTICLES
Published on Web 06/17/2005

Design, Synthesis, Linear, and Nonlinear Optical Properties of Conjugated (Porphinato)zinc(II)-Based Donor−Acceptor Chromophores Featuring Nitrothiophenyl and Nitrooligothiophenyl Electron-Accepting Moieties

Tian-Gao Zhang,[‡] Yuxia Zhao,[†] Inge Asselberghs,[†] André Persoons,[†] Koen Clays,*[,†] and Michael J. Therien*[,‡]

Contribution from the Center for Research on Molecular Electronics and Photonics, University of Leuven, B-3001 Leuven, Belgium, and Department of Chemistry, University of Pennsylvania, Philadelphia, Pennsylvania 19104-6323

Received November 16, 2004; E-mail: koen.clays@fys.kuleuven.ac.be; therien@sas.upenn.edu

Abstract: An extensive series of conjugated (porphinato)zinc(II)-based chromophores featuring nitrothiophenyl and nitrooligothiophenyl electron-accepting moieties has been synthesized using metal-catalyzed cross-coupling reactions involving [5-bromo-15-triisopropylsilylethynyl-10,20-diarylporphinato]zinc(II) and an unusual electron-rich Suzuki-porphyrin synthon, [5-(4-dimethylaminophenylethynyl)-15-(4′,4′,5′,5′-tetramethyl[1′,3′,2′]dioxaborolan-2′-yl)-10,20-diarylporphinato]zinc(II), with appropriately functionalized aryl and thienyl precursors. These donor−acceptor chromophores feature thiophenyl, [2,2′]bithiophenyl, and [2,2′;5′,2″]terthiophenyl units terminated with a 5-nitro group; one series of structures features these acceptor moieties appended directly to the porphyrin macrocycle *meso*-carbon position, while a second set utilizes an intervening *meso*-ethynyl moiety to modify porphyrin-to-thiophene conjugation. The dynamic hyperpolarizability of these compounds was determined from hyper-Rayleigh light scattering (HRS) measurements carried out at fundamental incident irradiation wavelengths (λ_{inc}) of 800 and 1300 nm; interestingly, measured β_{1300} values ranged from 650 → 4350 × 10^{-30} esu. The combined linear and nonlinear optical properties of these compounds challenge the classical concept of the nonlinearity/transparency tradeoff in charge-transfer chromophores: the magnitude of the molecular hyperpolarizability is observed to vary substantially despite approximately uniform ground-state absorptive signatures for a given porphyrin-to-thiophene linkage topology. These data show that these neutral dipolar molecules can express substantial β_{1300} values; such conjugated, electronically asymmetric porphyrin-thiophene chromophores may thus find utility for electrooptic applications at telecom-relevant wavelengths.

Introduction

Oligothiophenes, in which the thiophene units are linked through their respective α positions, have received much attention in recent years as electronic structural models for higher molecular weight polythiophenes, which have been extensively studied as both hole and electron transport materials.[1] In this regard, it is noteworthy that the first all-organic transistor was fabricated from sexithiophene;[2] as such, these conjugated structures constitute important electrooptic benchmarks for a wide range of organic semiconducting materials.

Likewise, the electronic structural properties of highly conjugated oligomeric porphyrin compounds suggest the potential for substantial charge mobility.[3−8] These data coupled with related optical properties[9−12] imply that porphyryl building blocks are attractive units from which to assemble a range of unusually polarizable and hyperpolarizable structures. Similarly, owing to the low resonance energy of the thiophene heterocycle,[13−19] thiophenes have found utility in a wide range of

[†] University of Leuven.
[‡] University of Pennsylvania.

(1) Fichou, D., Ed. *Handbook of Oligo- and Polythiophenes*; Wiley-VCH: Weinheim, 1999.
(2) Garnier, F.; Horowitz, G.; Peng, X. Z.; Fichou, D. *Adv. Mater.* **1990**, *2*, 592−594.
(3) Susumu, K.; Therien, M. J. *J. Am. Chem. Soc.* **2002**, *124*, 8550−8552.
(4) Lin, V. S. Y.; DiMagno, S. G.; Therien, M. J. *Science* **1994**, *264*, 1105−1111.
(5) Arnold, D. P.; Heath, G. A. *J. Am. Chem. Soc.* **1993**, *115*, 12197−12198.
(6) Wytko, J.; Berl, V.; McLaughlin, M.; Tykwinski, R. R.; Schreiber, M.; Diederich, F.; Boudon, C.; Gisselbrecht, J.-P.; Gross, M. *Helv. Chim. Acta* **1998**, *81*, 1964−1977.
(7) Taylor, P. N.; Huuskonen, J.; Rumbles, G.; Aplin, R. T.; Williams, E.; Anderson, H. L. *Chem. Commun.* **1999**, 909−910.
(8) Tsuda, A.; Osuka, A. *Science* **2001**, *293*, 79−82.
(9) Rubtsov, I. V.; Susumu, K.; Rubtsov, G. I.; Therien, M. J. *J. Am. Chem. Soc.* **2003**, *125*, 2687−2696.
(10) Kumble, R.; Palese, S.; Lin, V. S.-Y.; Therien, M. J.; Hochstrasser, R. M. *J. Am. Chem. Soc.* **1998**, *120*, 11489−11498.
(11) LeCours, S. M.; Guan, H.-W.; DiMagno, S. G.; Wang, C. H.; Therien, M. J. *J. Am. Chem. Soc.* **1996**, *118*, 1504−1510.
(12) Priyadarshy, S.; Therien, M. J.; Beratan, D. N. *J. Am. Chem. Soc.* **1996**, *118*, 1504−1510.
(13) Cook, M. J.; Katritzky, A. R.; Linda, P. In *Advances in Heterocyclic Chemistry*; Katritzky, A. R., Boulton, A. J., Eds.; Academic Press: New York, 1974; Vol. 17, pp 255−356.
(14) Breitung, E. M.; Shu, C.-F.; McMahon, R. J. *J. Am. Chem. Soc.* **2000**, *122*, 1154−1160.
(15) Dirk, C. W.; Katz, H. E.; Schilling, M. L.; King, L. A. *Chem. Mater.* **1990**, *2*, 700−705.
(16) Raimundo, J.-M.; Blanchard, P.; Gallego-Planas, N.; Mercier, N.; Ledoux-Rak, I.; Hierle, R.; Roncali, J. *J. Org. Chem.* **2002**, *67*, 205−218.

10.1021/ja0402553 CCC: $30.25 **© 2005 American Chemical Society**

nonlinear optical (NLO) materials.[16,20−34] Germane to this latter work are recent studies that examine the impact of terminal oligothiophene substituents on electrochemical and optical properties[35] and demonstrate that oligothiophene photophysical properties are particularly sensitive to substituent effects; for example, it has been established that the nitro functionality drives bathochromic shifts of the $S_0 \rightarrow S_n$ electronic transitions, large emission band Stokes shifts, and substantial solvatochromism. These established electrooptic properties suggest that such conjugated oligothiophenes may be effective in driving preferential excited-state electronic redistributions when used in combination with hyperpolarizable push−pull ethynylporphyrin structures.[11,12]

We report herein an extensive series of conjugated (porphinato)zinc(II)-based chromophores featuring nitro-thienyl electron-accepting moieties and (4-dialkylaminophenyl)ethynyl electron-releasing groups. These species were synthesized via metal-catalyzed cross-coupling reactions involving 5-bromo-15-triisopropylsilylethynyl-10,20-diarylporphinato]zinc(II) and an unusual electron-rich Suzuki-porphyrin synthon, [5-(4-dimethylaminophenylethynyl)-15-(4′,4′,5′,5′-tetramethyl[1′,3′,2′]-dioxaborolan-2′-yl)-10,20-diarylporphinato]zinc(II), with appropriately functionalized aryl, thiophenyl, and oligothiophenyl precursors. We describe the spectroscopic properties of these supermolecular NLO chromophores and frequency-dependent hyperpolarizabilities determined via hyper-Rayleigh light scattering (HRS) measurements. This combination of linear and nonlinear optical data suggests that these species are not only attractive platforms for developing electrooptic materials that function at long wavelength (1.3−1.5 μm) incident irradiation, but are unusual in that these chromophores do not exhibit the typical magnitude of hyperpolarizability/optical transparency tradeoffs common in such functional materials.

Experimental Section

Materials. Inert atmosphere manipulations were carried out under nitrogen prepurified by passage through an O_2 scrubbing tower (Schweizerhall R3−11 catalyst) and a drying tower (Linde 3-Å molecular sieves). Air-sensitive solids were handled in a Braun 150-M glovebox. Standard Schlenk techniques were employed to manipulate oxygen and moisture sensitive chemicals. Tetrahydrofuran (Fisher Scientific, HPLC grade) was distilled from potassium/benzophenone, while diethylamine and triethylamine were distilled from CaH_2. DMF (anhydrous), toluene (anhydrous), 1,2-dichloroethane (anhydrous), and *N*,*N*-diisopropylethylamine (redistilled, 99.5%) were used as received from Aldrich. $Pd(PPh_3)_4$ and CuI were obtained from either Aldrich or Strem. Tetrabutylammonium fluoride (TBAF; 1.0 M in THF), *N*-bromosuccinimide (NBS), TMEDA, HgO, $ZnCl_2$, $Zn(OAc)_2$, and Cs_2CO_3 (anhydrous) were obtained from Aldrich, while trimethylsilylacetylene was obtained from GFS Chemicals. Fuming HNO_3 (~90 wt %), acetic anhydride, glacial acetic acid, and iodine were obtained from Fisher. The thiophene-based organic reagents 2-bromo-5-nitrothiophene, 2-iodothiophene, thiophene, and 2,2′-bithiophene were purchased from Aldrich, while 2-ethynyl-5-nitrothiophene was synthesized via established methods.[23,36,37] 5,15-Bis[3,5-di-(3,3-dimethyl-1-butyloxy)phenyl]-porphyrin,[3] [5-bromo-10,20-bis(3,5-bis(3,3-dimethyl-1-butyloxy)phenyl)-porphinato]zinc(II)[3] (**porphyrin 1**), [5,15-dibromo-10,20-bis(3,5-bis(3,3-dimethyl-1-butyloxy)phenyl)porphinato]zinc(II)[3,38] (**porphyrin 2**), [5-(4′-dimethylaminophenylethynyl)-15-bromo-10,20-bis(3,5-bis(3,3-dimethyl-1-butyloxy)phenyl)porphinato]zinc(II)[11] (**porphyrin 4**), and [5-(4′,4′,5′,5′-tetramethyl[1′,3′,2′]dioxaborolan-2′-yl)-10,20-bis(3,5-bis(3,3-dimethyl-1-butyloxy)phenyl)porphinato]zinc(II)[39] (**porphyrin 5**) were prepared using methods similar to that reported previously.

^{1}H NMR spectra were recorded on either a Brüker AC-250 or Brüker AM-360 spectrometer. All chemical shifts for ^{1}H NMR spectra are relative to that of TMS unless otherwise noted. All *J* values are reported in Hertz. The number of attached protons is found in parentheses following the chemical shift value. Chromatographic purification (silica gel 60, 230−400 mesh, EM Scientific; Bio-Beads S-X1, Bio-Rad Laboratories) of all newly synthesized compounds was accomplished on the benchtop. MALDI-TOF mass spectroscopic data were obtained with either an Applied Biosystems Perceptive Voyager-DE instrument in the Laboratories of Dr. Virgil Percec (Department of Chemistry, University of Pennsylvania) or a PerSpective BioSystems Voyager-DE instrument in the Laboratories of Dr. William DeGrado (Department of Biochemistry and Biophysics, University of Pennsylvania School of Medicine). Samples were prepared as micromolar solutions in THF, and either dithranol (Aldrich) or α-cyano-4-hydroxy cinnamic acid (α-CHCA) was utilized as the matrix. FAB data was obtained in the Drexel Mass Spectrometry facility. Electrospray ionization (ESI-MS) and chemical ionization (CI-MS) data were obtained in the University of Pennsylvania Chemistry Mass Spectrometry Facility.

Instrumentation. Electronic spectra were recorded on an OLIS UV/vis/near-IR spectrophotometry system that is based on the optics of a Cary 14 spectrophotometer. Emission spectra were recorded on a SPEX Fluorolog luminescence spectrophotometer that utilized a T-channel configuration with a red sensitive R2658 Hamamatsu PMT and liquid nitrogen cooled InGaAs detector; these spectra were corrected using the spectral output of a calibrated light source supplied by the National Bureau of Standards. Time-correlated single photon counting (TCSPC) spectroscopic measurements were performed at the Regional Laser and Biotechnology Laboratory (RLBL) at the University of Pennsylvania using an instrument described previously;[40] these data were analyzed using Lifetime (RLBL) and Globals Unlimited (LFD, University of Illinois) Programs.

(17) Wheland, G. W. *Resonance in Organic Chemistry*; Wiley: New York, 1955.
(18) Smith, M. B.; March, J. *March's Advanced Organic Chemistry: Reactions, Mechanisms, and Structure*, 5th ed.; Wiley: New York, 2001.
(19) Waite, J.; Papadopoulos, M. G. *J. Phys. Chem.* **1990**, *94*, 6244−6249.
(20) He, M.; Leslie, T. M.; Sinicropi, J. A. *Chem. Mater.* **2002**, *14*, 4662−4668.
(21) Bedworth, P. V.; Cai, Y.; Jen, A.; Marder, S. R. *J. Org. Chem.* **1996**, *61*, 2242−2246.
(22) Cai, C.; Liakatas, I.; Wong, M.-S.; Bosch, M.; Bosshard, C.; Gunter, P.; Concilio, S.; Tirelli, N.; Suter, U. W. *Org. Lett.* **1999**, *1*, 1847−1849.
(23) Mueller, T. J. J.; Robert, J. P.; Schmaelzlin, E.; Braeuchle, C.; Meerholz, K. *Org. Lett.* **2000**, *2*, 2419−2422.
(24) Kim, O.-K.; Fort, A.; Barzoukas, M.; Blanchard-Desce, M.; Lehn, J.-M. *J. Mater. Chem.* **1999**, *9*, 2227−2232.
(25) Ledoux, I.; Zyss, J.; Jutand, A.; Amatore, C. *Chem. Phys.* **1991**, *150*, 117−123.
(26) Rao, V. P.; Jen, A. K. Y.; Wong, K. Y.; Drost, K. J. *Chem. Commun.* **1993**, 1118−1120.
(27) Rao, V. P.; Jen, A. K. Y.; Wong, K. Y.; Drost, K. J. *Tetrahedron Lett.* **1993**, *34*, 1747−1750.
(28) Rao, V. P.; Cai, Y. M.; Jen, A. K. Y. *Chem. Commun.* **1994**, 1689−1690.
(29) Wong, K. Y.; Jen, A. K. Y.; Rao, V. P.; Drost, K. J. *J. Chem. Phys.* **1994**, *100*, 6818−6825.
(30) Illien, B.; Jehan, P.; Botrel, A.; Darchen, A.; Ledoux, I.; Zyss, J.; Le Magueres, P.; Ouahab, L. *New J. Chem.* **1998**, *22*, 633−641.
(31) Chou, S. S. P.; Hsu, G. T.; Lin, H. C. *Tetrahedron Lett.* **1999**, *40*, 2157−2160.
(32) Brasselet, S.; Cherioux, F.; Audebert, P.; Zyss, J. *Chem. Mater.* **1999**, *11*, 1915−1920.
(33) Varanasi, P. R.; Jen, A. K. Y.; Chandrasekhar, J.; Namboothiri, I. N. N.; Rathna, A. *J. Am. Chem. Soc.* **1996**, *118*, 12443−12448.
(34) Albert, I. D. L.; Morley, J. O.; Pugh, D. *J. Phys. Chem.* **1995**, *99*, 8024−8032.
(35) Garcia, P.; Pernaut, J. M.; Hapiot, P.; Wintgens, V.; Valat, P.; Garnier, F.; Delabouglise, D. *J. Phys. Chem.* **1993**, *97*, 513−516.
(36) Xia, A.; Selegue, J. P. *Inorg. Chim. Acta* **2002**, *334*, 219−224.
(37) Vegh, D.; Kovac, J.; Dandarova, M. *Tetrahedron Lett.* **1980**, *21*, 969−970.
(38) DiMagno, S. G.; Lin, V. S. Y.; Therien, M. J. *J. Org. Chem.* **1993**, *58*, 5983−5993.
(39) Hyslop, A. G.; Kellett, M. A.; Iovine, P. M.; Therien, M. J. *J. Am. Chem. Soc.* **1998**, *120*, 12676−12677.
(40) Holtom, G. R. *SPIE* **1990**, *1204*, 1.

Hyper-Rayleigh Light Scattering (HRS) Measurements. Femtosecond HRS experiments were performed at 800[41] and 1300 nm.[42] The chromophores were dissolved in THF and passed through 0.2 μm filters. Crystalviolet chloride (CV, 338 $\times$ 10^{-30} esu in CH_3OH) and disperse red 1 (DR1, 54 $\times$ 10^{-30} esu in $CHCl_3$) were utilized as reference chromophores at 800 and 1300 nm, respectively. For these external references in different solvents, standard local field correction factors were applied [$((n_D^2 + 2)/3)^3$ where n_D is the refractive index of the solvent at the sodium D line]. Note that these experiments were performed at low chromophore concentrations [$<4 \times 10^{-5}$ M^{-1} (800 and 1300 nm)]; the linearity of the HRS signal as a function of chromophore concentration confirmed that no significant self-absorption of the second harmonic generation (SHG) signal occurred in these experiments. HRS signals measured for the dipolar 5,15-disubstituted-(porphinato)zinc(II) chromophores were analyzed as resulting from a single major hyperpolarizability tensor component, i.e., the diagonal component β_{zzz} along the molecular *z*-axis, which corresponds in the molecular reference frame to the axis of highest conjugation. The reference chromophores CV and DR1 were treated as benchmark octopolar and dipolar chromophores, respectively.

Nonlinear Optical Chromophores. Synthetic details and characterization data for: 5-nitro-[2,2′]bithiophene (**1**), 5′-iodo-5-nitro-[2,2′]-bithiophene (**2**), 5′-trimethylsilylethynyl-5-nitro-[2,2′]bithiophene (**3**), 5′-ethynyl-5-nitro-[2,2′]bithiophene (**4**), 2-iodo-5-nitro-thiophene (**5**), 5-nitro-[2,2′;5′,2″]terthiophene (**6**), 5″-iodo-5-nitro-[2,2′;5′,2″]terthiophene (**7**), 5″-ethynyl-5-nitro-[2,2′;5′,2″]terthiophene (**8**), [5-(4′-dimethylaminophenylethynyl)-10,20-bis[3′,5′-bis(3″,3″-dimethyl-1″-butyloxy)phenyl]porphinato]zinc(II) (**porphyrin 3**), [5-(4-dimethylaminophenylethynyl)-15-(4′,4′,5′,5′-tetramethyl[1′,3′,2′]dioxaborolan-2′-yl)-10,20-bis(3,5-bis(3,3-dimethyl-1-butyloxy)phenyl)porphinato]zinc(II) **(porphyrin 6)**, [5-(4-dimethylaminophenylethynyl)-15-(5-nitrothien-2-yl)-10,20-bis(3,5-bis(3,3-dimethyl-1-butyloxy)phenyl)porphinato]-zinc(II) (**porphyrin 7**), [5-(4-dimethylaminophenylethynyl)-15-[5-nitro-[2,2′]bithien-5′-yl)-10,20-bis(3,5-bis(3,3-dimethyl-1-butyloxy)phenyl)-porphinato]zinc(II) (**porphyrin 8**), [5-(4-dimethylaminophenylethynyl)-15-[5-nitro-[2,2′;5′,2″]terthien-5″-yl)-10,20-bis(3,5-bis(3,3-dimethyl-1-butyloxy)phenyl)porphinato]zinc(II) (**porphyrin 9**), [5-[4′-dimethylaminophenylethynyl]-15-[(5-nitrothienyl-2-ethynyl]-10,20-bis[3′,5′-bis(3″,3″-dimethyl-1″-butyloxy)phenyl]porphinato]zinc(II) (**porphyrin 10**), [5-[4′-dimethylaminophenylethynyl]-15-[5-nitro-[2,2′]bithienyl-5′-ethynyl]-10,20-bis[3′,5′-bis(3″,3″-dimethyl-1″-butyloxy)phenyl]porphinato]zinc(II) (**porphyrin 11**), [5-[4′-dimethylaminophenylethynyl]-15-[5-nitro-[2,2′;5′,2″]terthienyl-5″-ethynyl]-10,20-bis[3′,5′-bis(3″,3″-dimethyl-1″-butyloxy)phenyl]porphinato]zinc(II) (**porphyrin 12**), and [5-(5′-nitro-2′-thienyl)-10,20-bis(3″,5″-bis(3,3-dimethyl-1-butyloxy)-phenyl)porphinato]zinc(II) (**porphyrin 13**) are provided in the Supporting Information.

Results and Discussion

Design and Synthesis. The energetic proximity of oligothiophene frontier orbital energy levels to those of porphyrinoid compounds has motivated the synthesis of a variety of thiophene-derivatized conjugated macrocycles. While the synthesis of symmetrically substituted tetrakis(*meso*-2-thienyl)porphyrin was first reported in 1968,[43] syntheses of asymmetrically substituted *meso*-(oligo)thienyl porphyrins were only realized recently.[44] The limited examples[44−46] of these structures derive from Lindsey's hybrid condensation methodology,[47] which exploit (oligo)thiophene-derived aldehyde compounds synthesized from multistep reactions, pyrrollic synthons, and another selected organic aldehyde. Drawbacks of this method when applied to asymmetric porphyrin synthesis often include low statistical yields of the desired compound, as well as potentially arduous purification and separation.

Modern metal-catalyzed bond-forming reactions have enabled straightforward elaboration of functionality at the porphyrin macrocycle *meso* and β positions[38,39,48,49] and have facilitated the fabrication of supramolecular porphyrin-based assemblies[3,4,50,51] and new electrooptic materials.[11,52−55] Because highly conjugated hyperpolarizable structures that contain porphyrinoid and oligothiophene components will likely feature significant electronic asymmetry, metal-catalyzed cross-coupling methodologies provide a general route into such structures. Schemes 1−4 show that the combination of an electron-rich Suzuki-porphyrin synthon, [5-(4-dimethylaminophenylethynyl)-15-(4′,4′,5′,5′-tetramethyl[1′,3′,2′]dioxaborolan-2′-yl)-10,20-diarylporphinato]zinc(II), [5-bromo-15-triisopropylsilylethynyl-10,20-diarylporphinato]zinc(II),[39] (4-dialkylaminophenyl)ethyne, and a variety of appropriately functionalized nitrothienyl precursors can be utilized in Pd-catalyzed cross-coupling reactions to derive a large family of such hyperpolarizable chromophores.

Oligothiophenes bearing electron-releasing or -accepting groups[35,56] have featured in structures that probe intramolecular electronic and energy transfer reactions[44,46] as well as an extensive family of hyperpolarizable chromophores.[16,22−34] Studies that examined the impact of terminal oligothiophene substituents on electrochemical and optical properties[35] demonstrate that nitro functionality drives bathochromic shifts of the $S_0 \rightarrow S_n$ electronic transitions, large emission band Stokes shifts, and substantial solvatochromism. While these terminally nitro-substituted oligothiophenes have previously been synthesized and examined mainly for their potential utility as phototoxic agents,[57−61] their electronic structural properties suggest that such conjugated oligothiophenes may find utility in driving preferential excited-state electronic redistributions within a hyperpolarizable push−pull ethynylporphyrin structural motif.[11,12]

(41) Olbrechts, G.; Strobbe, R.; Clays, K.; Persoons, A. *Rev. Sci. Instrum.* **1998**, *69*, 2233−2241.
(42) Olbrechts, G.; Wostyn, K.; Clays, K.; Persoons, A. *Opt. Lett.* **1999**, *24*, 403−405.
(43) Treibs, A.; Haeberle, N. *Justus Liebigs Ann. Chem.* **1968**, *718*, 183−207.
(44) Wuerthner, F.; Vollmer, M. S.; Effenberger, F.; Emele, P.; Meyer, D. U.; Port, H.; Wolf, H. C. *J. Am. Chem. Soc.* **1995**, *117*, 8090−8099.
(45) Vollmer, M. S.; Wurthner, F.; Effenberger, F.; Emele, P.; Meyer, D. U.; Stumpfig, T.; Port, H.; Wolf, H. C. *Chem.—Eur. J.* **1998**, *4*, 260−269.
(46) Ikemoto, J.; Takimiya, K.; Aso, Y.; Otsubo, T.; Fujitsuka, M.; Ito, O. *Org. Lett.* **2002**, *4*, 309−311.
(47) Lindsey, J. S. In *Metalloporphyrins Catalyzed Oxidations*; Montanari, F., Casella, L., Eds.; Kluwer: Dordrecht, 1994; Vol. 17, pp 49−86.
(48) DiMagno, S. G.; Lin, V. S. Y.; Therien, M. J. *J. Am. Chem. Soc.* **1993**, *115*, 2513−2515.
(49) Fletcher, J. T.; Therien, M. J. *J. Am. Chem. Soc.* **2000**, *122*, 12393−12394.
(50) Lin, V. S.-Y.; Therien, M. J. *Chem.—Eur. J.* **1996**, *1*, 645−651.
(51) Lin, V. S.-Y.; Iovine, P. M.; DiMagno, S. G.; Therien, M. J. *Inorg. Synth.* **2002**, *33*, 55−61.
(52) Zhang, T.-G.; Therien, M. J. *Abstracts of Papers of 220th ACS National Meeting*; American Chemical Society: Washington, DC, United States, 2000; pp INOR-374.
(53) Zhang, T.-G.; Therien, M. J. *Polym. Prepr. (Am. Chem. Soc., Div. Polym. Chem.)* **2002**, *43*, 570−571.
(54) Uyeda, H. T.; Zhao, Y.; Wostyn, K.; Asselberghs, I.; Clays, K.; Persoons, A.; Therien, M. J. *J. Am. Chem. Soc.* **2002**, *124*, 13806−13813.
(55) Zhang, T.-G. Ph.D. Thesis, University of Pennsylvania, 2003.
(56) Casado, J.; Pappenfus, T. M.; Miller, L. L.; Mann, K. R.; Orti, E.; Viruela, P. M.; Pou-Amerigo, R.; Hernandez, V.; Lopez Navarrete, J. T. *J. Am. Chem. Soc.* **2003**, *125*.
(57) Eachern, A. M.; Soucy, C.; Leitch, L. C.; Arnason, J. T.; Morand, P. *Tetrahedron* **1988**, *44*, 2403−2412.
(58) Soucy-Breau, C.; MacEachern, A.; Leitch, L. C.; Arnason, T.; Morand, P. *J. Heterocycl. Chem.* **1991**, *28*, 411−416.
(59) Marles, R. J.; Arnason, J. T.; Compadre, R. L.; Compadre, C. M.; Soucy-Breau, C.; Mehta, B.; Morand, P.; Redmond, R. W.; Scaiano, J. C. *Recent Advances in Phytochemistry*; 1991; Vol. 25, pp 371−396.
(60) Marles, R. J.; Hudson, J. B.; Graham, E. A.; Soucy-Breau, C.; Morand, P.; Compadre, R. L.; Compadre, C. M.; Towers, G. H. N.; Arnason, J. T. *Photochem. Photobiol.* **1992**, *56*, 479−487.
(61) D'Auria, M.; Mauriello, G. *Photochem. Photobiol.* **1994**, *60*, 542−545.

Scheme 1. Synthesis of Key Oligothiophene Precursors[a]

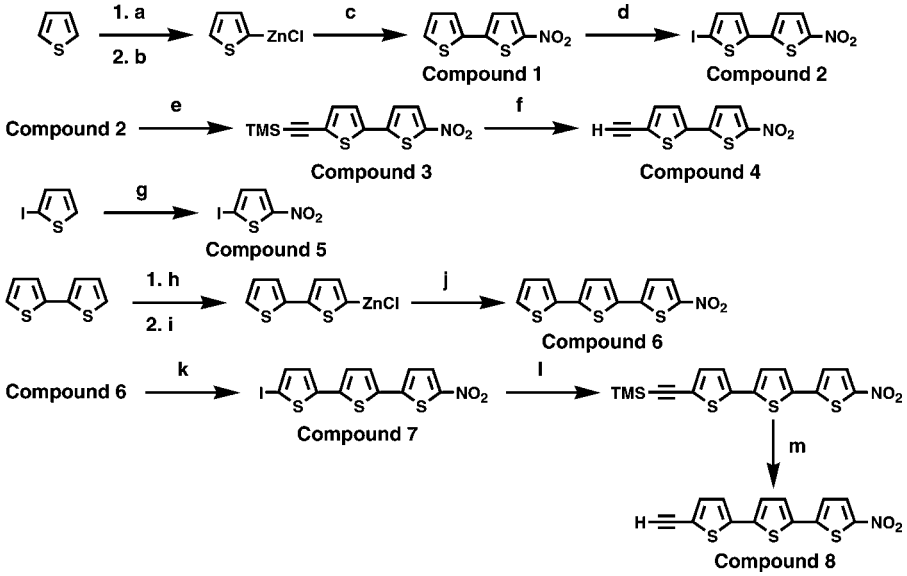

[a] Conditions: (a) *n*-BuLi, TMEDA, THF, −78 °C; (b) $ZnCl_2$, THF; (c) 2-bromo-5-nitrothiophene, $Pd(PPh_3)_4$, THF; (d) I_2, HgO, HOAc, DMF, $CHCl_3$; (e) trimethylsilylethyne, $Pd(PPh_3)_4$, CuI, $(i\text{-Pr})_2NH$, DMF, $CHCl_3$; (f) KOH, MeOH; (g) fuming HNO_3, Ac_2O; (h) *n*-BuLi, TMEDA, THF, −78 °C; (i) $ZnCl_2$, THF; (j) 2-iodo-5-nitrothiophene, $Pd(PPh_3)_4$, THF; (k) I_2, HgO, HOAc, DMF, $CHCl_3$; (l) trimethylsilylethyne, $Pd(PPh_3)_4$, CuI, $(i\text{-Pr})_2NH$, DMF, $CHCl_3$; (m) KOH, MeOH.

Scheme 2. Synthesis of Porphyrin-Based Organometallic Reagents Where Boronic Esters Are Appended to a (Porphinato)zinc(II) Framework[a]

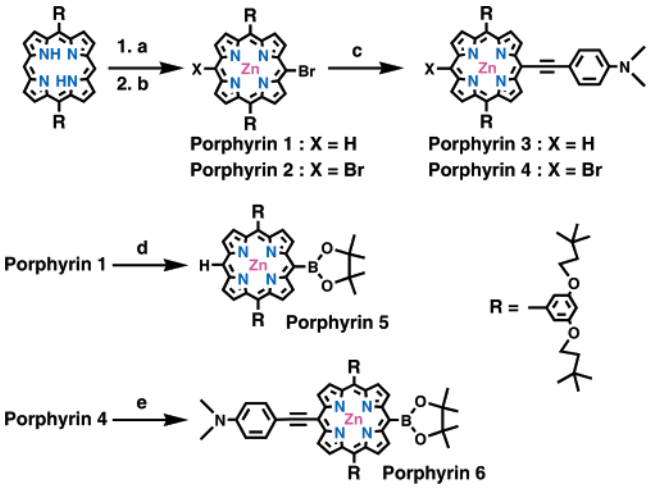

[a] Conditions: (a) NBS, $CHCl_3$; (b) $Zn(OAc)_2$, $CHCl_3$; (c) 4-dimethylaminophenylethyne, $Pd(PPh_3)_4$, CuI, THF, Et_2NH; (d and e) pinacolborane, $Pd(PPh_3)_2Cl_2$, Et_3N, 1,2-dichloroethane.

Scheme 1 shows the synthetic route utilized to fabricate terminally nitro-substituted thiophene and oligothiophene moieties having reactive iodo or ethynyl functionality that enable facile conjugation to the porphyrin *meso*-carbon position. These electron-poor thiophene species enable the synthesis of (porphinato)zinc(II)-to-thiophenyl linkage topologies that comprise both a direct carbon−carbon single bond and conjugation through an intervening ethynyl unit (Schemes 2−4).

Scheme 2 highlights two functionalized porphyrinic building blocks, **porphyrins 4** and **5**, that are structurally related to previously reported synthons:[11,39] these species feature 10- and 20-(3,3-dimethyl-1-butyloxy)phenyl groups and define more soluble analogues of ring-metalated [5-(4′,4′,5′,5′-tetramethyl-[1′,3′,2′]dioxaborolan-2′-yl)-10,20-diphenylporphinato]zinc(II)[39] and the [5-bromo-15-arylethynylporphinato]zinc(II) compound that provided the synthetic entry point into the originally reported hyperpolarizable, push−pull arylethynylporphyrin systems.[11,12] **Porphyrin 6** (Scheme 2) is related to these structures, combining both organometallic and arylethynyl functionalities; this electron-rich, electronically asymmetric porphyrylboronate complex is a valuable precursor for the fabrication of (porphinato)zinc(II) chromophores in which thiophene and oligothiophene units are directly linked to the macrocycle *meso* position (Scheme 3). Note that the 4,4,5,5-tetramethyl-[1,3,2]dioxaborolan-2-yl moiety is electron-withdrawing in nature (Hammett σ_p, value for $B(OH)_2 = 0.12$);[62] as such, its electronic absorption spectral characteristics (Figure 1) resemble those delineated for electronically asymmetric (5,15-arylethynylporphinato)metal complexes that feature substantial charge resonance character.[11,12]

The corresponding thiophene derivatives highlighted in Schemes 3 and 4 were prepared using modified literature methods. 2-Iodo-5-nitrothiophene[61] was prepared through the electrophilic nitration of 2-iodothiophene with fuming nitric acid at low temperature with good yield and regioselectivity. 5-Nitro-[2,2′;5′,2″]terthiophene,[58] synthesized previously through the electrophilic nitration of [2,2′;5′,2″]terthiophene with fuming nitric acid, suffers from purification problems associated with modest regioselectivity and multinitration. For the synthetic targets of Schemes 2 and 3, we adopted a modified literature procedure[63] using palladium-catalyzed Negishi cross-coupling protocols to synthesize the 5-nitro-[2,2′;5′,2″]terthiophene from 2-iodo-5-nitrothiophene and the organozinc derivative of bithiophene; subsequent iodination with iodine/HgO afforded the reactive synthon 5″-iodo-5-nitro-[2,2′;5′,2″]terthiophene (see Supporting Information).

Linear Optical Properties. Table 1 displays steady-state absorption and fluorescence emission data for nitro- and iodo-functionalized thiophenes and oligothiophenes; tabulated here

(62) Hansch, C.; Leo, A.; Taft, R. W. *Chem. Rev.* **1991**, *91*, 165−195.
(63) Ibrahim, M. A.; Lee, B.-G.; Park, N.-G.; Pugh, J. R.; Eberl, D. D.; Frank, A. J. *Synth. Met.* **1999**, *105*, 35−42.

Scheme 3. Synthesis of Porphyrin Chromophores that Feature Nitro-Functionalized Thiophene and Oligothiophene Electron-Accepting Moieties

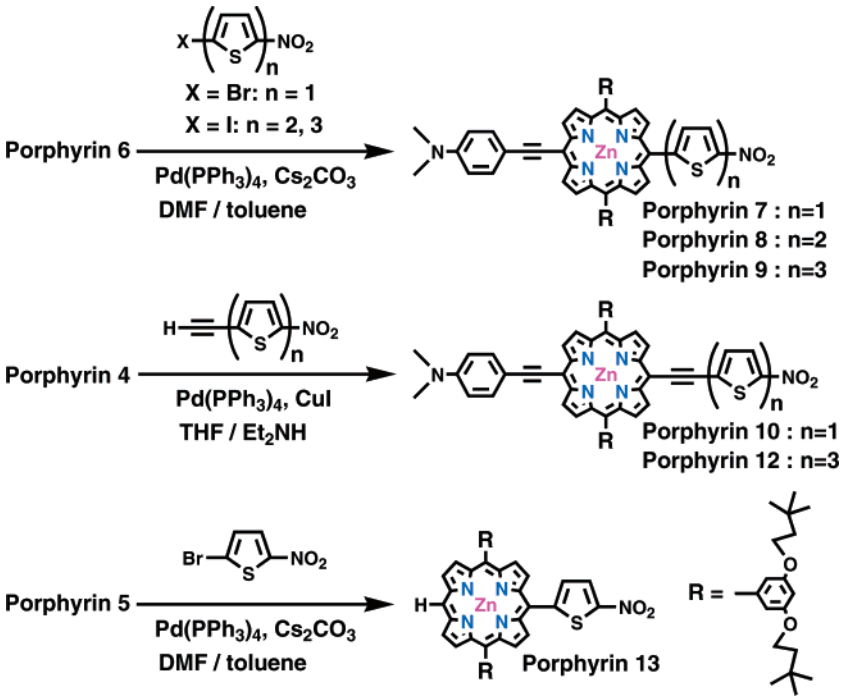

Scheme 4. Synthesis of a Porphyrin Chromophore with a 5-Nitro-[2,2′]bithienyl-5′-ethynyl Acceptor Moiety

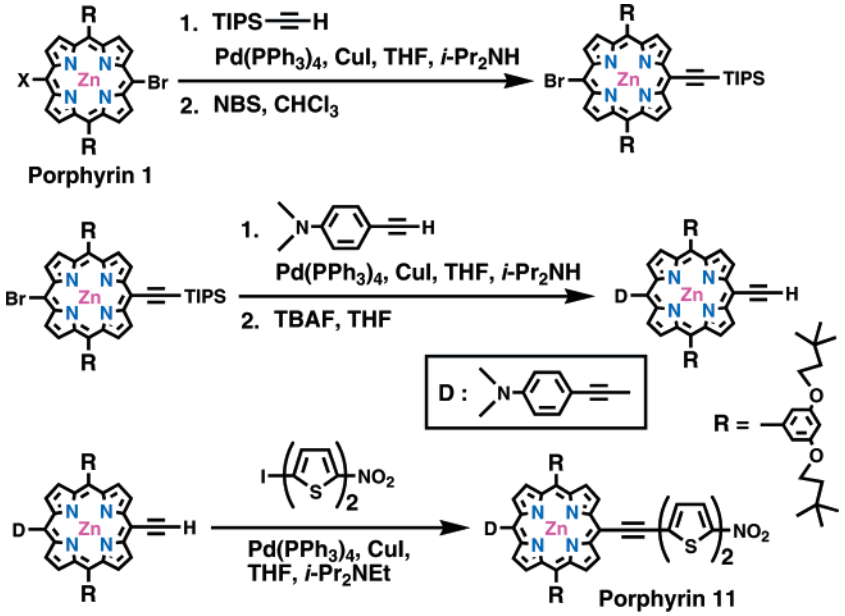

as well for comparative purposes are analogous data for thiophene, [2,2′]bithiophene, and [2,2′;5′,2″]terthiophene benchmarks.[64,65] Consistent with both experimental and theoretical studies of simple oligothiophenes,[64,66] the fluorescence emission and absorption maxima of functionalized oligothiophenes follow a reciprocal dependence upon chain length (Supporting Information) over modest oligomer lengths.[67] The substitution of a nitro group at one of the terminal α positions in α-oligothiophenes leads to a significant bathochromic shift of the prominent absorption and fluorescence emission bands (Table 1). Appending a second conjugating terminal ethynyl or iodo moiety, in addition to the terminal nitro group, leads to more pronounced shifts of these transitions to lower energy in the α-oligothiophenes.

The linear optical properties of the six (porphinato)zinc(II)-based chromophores featuring nitrothiophenyl and nitrooligothiophenyl electron-accepting moieties are summarized in Table 2.

General linear optical characteristics (Table 2) of these chromophores worth noting include the facts that the Q-band

(64) Chosrovian, H.; Rentsch, S.; Grebner, D.; Dahm, D. U.; Birckner, E.; Naarmann, H. *Synth. Met.* **1993**, *60*, 23−26.
(65) Inoue, S.; Jigami, T.; Nozoe, H.; Aso, Y.; Ogura, F.; Otsubo, T. *Heterocycles* **2000**, *52*, 159−170.
(66) Egelhaaf, H.-J.; Oelkrug, D.; Gebauer, W.; Sokolowski, M.; Umbach, E.; Fischer, T.; Bauerle, P. *Opt. Mater. (Amsterdam)* **1998**, *9*, 59−64.
(67) Becker, R. S.; de Melo, J. S.; Macanita, A. L.; Elisei, F. *J. Phys. Chem.* **1996**, *100*, 18683−18695.

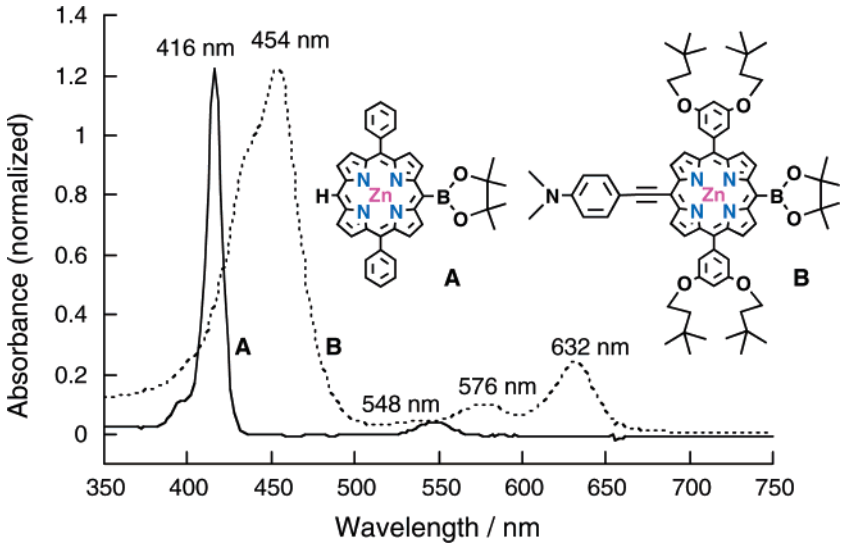

Figure 1. Comparative absorption spectra in THF solvent of ring-metalated [5-(4′,4′,5′,5′-tetramethyl-[1′,3′,2′]dioxaborolan-2′-yl)-10,20-diphenylporphinato]-zinc(II) and **porphyrin 6**, an electronically asymmetric porphyrylboronate complex that features an electron-releasing *meso*-(4′-dimethylaminophenylethynyl) group.

Table 1. Steady-State Absorption and Fluorescence Emission Data for Nitro- and Iodo-Functionalized Thiophenes and Oligothiophenes Relative to Benchmark Structures[35,64,65,67,96] in THF Solvent

Precursors	λ_{Abs}^{max} (nm)	ν_{max} (cm^{-1})	λ_{em} (nm)	ν_{em} (cm^{-1})	Stokes Shift (cm^{-1})
	230	43478	N.F.	N.F.	N/A
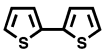	304	32895	361	27701	5194
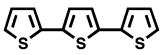	353	28329	431	23202	5127
	312	32051	344	29070	2982
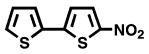	394	25381	478	20921	4460
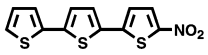	434	23041	576	17361	5580
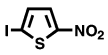	340	29412	354	28249	1163
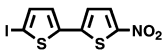	402	24876	500	20000	4876
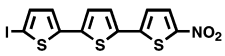	440	22727	581	17212	5516
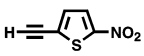	340	29412	N.F.	N.F.	N/A
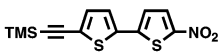	410	24390	502	19920	4470
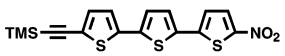	441	22676	581	17212	5464

[a] Only absorption and emission band maxima are tabulated. N.F. = nonfluorescent; N/A = not applicable or not available.

absorption maxima, emission energy, and $E_{0,0}$ (determined from the spectral overlap of the absorption and emission bands) depend chiefly on whether the thiophene or oligothiophene unit is linked to the porphyrin macrocycle *meso*-carbon position (**porphyrins 7**−**9**) or via an intervening ethynyl moiety (**porphyrins 10**−**12**). The Stokes shifts for these compounds vary

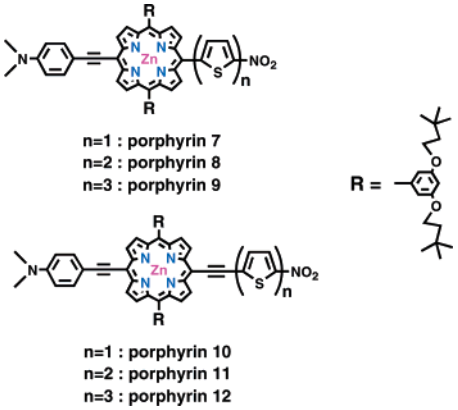

from 350 to 1300 cm^{-1}, indicating that these nitrothiophenyl- and nitrooligothiophenyl-derivatized [5-(4′-dimethylaminophenylethynyl)porphinato]zinc(II) chromophores undergo modest-to-substantial excited-state electronic structural redistributions. These Stokes shift data are consistent with expectations based on analogous studies of α-oligothiophene electronic structure which suggest an excited state having substantial quinoidal character.[64,67−69] The quinoidal resonance form enhances the extent to which electron density is redistributed between the electron-releasing and electron-accepting components of chromophores **7**−**12**. Augmenting electronic coupling between chromophore donor and acceptor moieties in the excited state relative to the ground state provides a mechanism by which chromophore second-order nonlinear optical properties may be enhanced (vide infra).

Note that, for each mode of connectivity, the chromophores that incorporate a single thiophene unit (**porphyrins 7** and **10**) possess the largest Stokes shifts within their respective structural classes. Consistent with this observation, normalized emission spectral data (Figure 2) indicate that **7** and **10** possess the longest wavelength emission maxima [λ_{em}(max)] for chromophores possessing nitrothiophenyl and nitrooligothiophenyl units linked respectively to the porphyrin *meso* position via direct single bonds and ethynyl groups. Further, it is evident that **porphyrins 7** and **10** possess the greatest degree of excited-state electronic structural heterogeneity; note that the steady-state emission spectra of these species exhibit the largest spectral breadths (Figure 2) within their respective structural classes, consistent with the notion that these chromophores manifest both the largest porphyrin-to-thiophene interplanar torsional angle distributions and significant conformeric populations that possess extensive porphyrin-thiophene conjugation.

For simple α-oligothiophenes, the excited-state electronic structure is known to feature a substantial contribution of the corresponding quinoidal resonance form.[64,67−69] This α-oligothiophene electronic structural feature coupled with good matching of (porphinato)zinc(II) and α-oligothiophene frontier orbital energy levels drives the expectation that the terminal nitro group of **porphyrins 7**−**12** conjugates more effectively with the porphyrin macrocycle in the S_1 state than in the S_0 state (Figure 2 and Table 2). Consistent with this, Figure 3 shows

Table 2. Linear and Nonlinear Optical Data for Porphyrin Chromophores **7**−**12** in THF Solvent

porphyrin chromophore	no. of thiophene rings (*n*)	Soret band (nm)	Q band λ_{max} (nm)	emission λ_{max} (nm)	$E_{0,0}$ (eV)	Stokes shift (cm^{-1})	β_{800nm} (10^{-30} esu)	β_{1300nm} (10^{-30} esu)
7	1	456	580, 640	698	1.85	1298	480	2400
8	2	457	583, 641	669	1.89	653	345	2200
9	3	458	579, 641	662	1.90	495	510	4350
10	1	465	685	714	1.77	593	860	690
11	2	468	683	706	1.78	477	N/A	670
12	3	470	683	700	1.79	356	N/A	1170

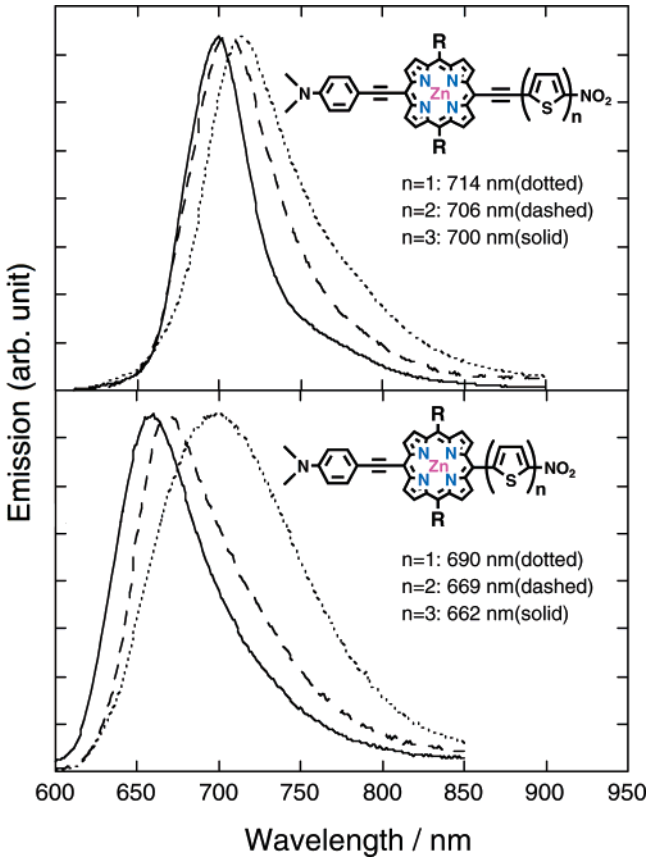

Figure 2. Comparative normalized emission spectra for donor−acceptor porphyrin chromophores where thiophene and oligothiophene units are linked to the macrocycle *meso*-carbon position by (A) a carbon−carbon single bond (**porphyrins 7**−**9**) and (B) via an intervening ethynyl moiety (**porphyrins 10**−**12**). Experimental conditions: solvent = THF, T = 293 K.

representative electronic spectral data for **porphyrin 3**, 5″-ethynyl-5-nitro-[2,2′;5′,2″]terthiophene, and **porphyrin 12**; these spectra underscore the supermolecular character of the composite **porphyrin 12** electronic states.

Nonlinear Optical Properties. Optimizing chromophore second-order nonlinear optical properties has focused primarily on engineering the electronic nature of electron donor (D) and acceptor (A), and the conjugation length of the organic bridge that links these units. The former controls D−A mixing with respect to a specific bridge, while the latter plays a role in modulating D−A electronic coupling as well as determines the magnitude of the change in dipole moment. For example, increasing the magnitude of the ground-to-excited state change in dipole moment by bridge conjugation length augmentation typically diminishes the square of the dipole matrix element and augments the square of the CT transition energy; the latter

(68) Odobel, F.; Suresh, S.; Blart, E.; Nicolas, Y.; Quintard, J.-P.; Janvier, P.; Le Questel, J.-Y.; Illien, B.; Rondeau, D.; Richomme, P.; Haupl, T.; Wallin, S.; Hammarstrom, L. *Chem.*−*Eur. J.* **2002**, *8*, 3027−3046.
(69) Pappenfus, T. M.; Raff, J. D.; Hukkanen, E. J.; Burney, J. R.; Casado, J.; Drew, S. M.; Miller, L. L.; Mann, K. R. *J. Org. Chem.* **2002**, *67*, 6015−6024.

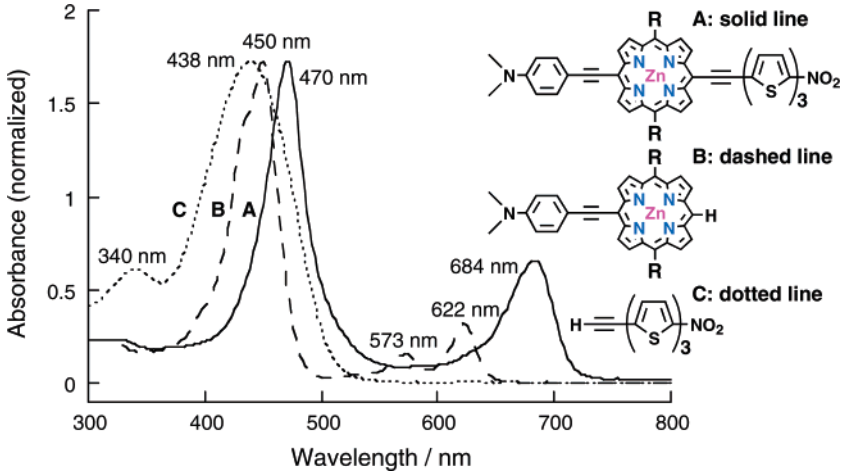

Figure 3. Comparative steady-state absorption spectra of **porphyrin 3**, 5″-ethynyl-5-nitro-[2,2′;5′,2″]terthiophene, and **porphyrin 12** recorded in THF solvent.

two effects have their genesis in the fact that increased bridge lengths abate D−A electronic coupling. Maximizing the molecular first hyperpolarizability, β, thus involves a subtle interplay between three parameters that do not necessarily simultaneously attain their optimal value for a particular molecular structure (D, A, bridge); hence, optimization of the magnitude of β for a given chromophoric structural class generally involves a balancing act.[70,71] Nonlinear optical chromophore design strategies that utilize structures where (i) a significant portion of the oscillator strength of the charge transfer transition that couples D to A is bridge-localized, (ii) the CT transition dipole is oriented directly along the D-to-A molecular charge transfer axis, and (iii) low-lying electronically excited states possess enhanced electronic delocalization with respect to the ground state provide an alternative approach to engineering large molecular first hyperpolarizabilities, as augmented D−A distances would not necessarily track with diminished CT oscillator strengths and correspondingly increased transition energies. This design approach has been discussed in detail previously.[11,12] These notions, coupled with the facts that (i) α-oligothiophene excited-state electronic structure features a substantial quinoidal resonance form contribution[64,67−69] and (ii) α-oligothiophene frontier orbital energy levels lie in close proximity to those of porphyrinoid compounds, motivated the syntheses of **porphyrins 7−12**.

For these dipolar molecules, the diagonal component β_{zzz} of the molecular first hyperpolarizability (or second-order nonlinear polarizability) tensor has been evaluated (see Experimental Section). The molecular first hyperpolarizability, β, was evaluated by hyper-Rayleigh scattering (HRS) measurements for chromophores **7−12** in solution.[72,73] For these compounds that show fluorescence, it is essential to use a femtosecond (fs) pulsed laser in these experiments in order to discriminate between scattering (immediate and hyper-Rayleigh) and time-delayed, multiphoton fluorescence. Our approach for eliminating a multiphoton contribution to the HRS signal involves a Fourier transform of the frequency domain data to the time domain. As the fluorescence is to a large extent delayed in time, it is advantageous to measure the HRS signal at early times following the incident fundamental laser pulse.[74] In the frequency domain, this results in any fluorescence signals being phase shifted, and diminished in amplitude with increasing amplitude modulation (AM) frequencies.[41,75] Such fs HRS measurements of fluorescing molecules that discriminate between scattering and multiphoton fluorescence are performed at successively higher AM frequencies. The analysis of the frequency-dependent *apparent* hyperpolarizability data provides a true (fluorescence-free) hyperpolarizability value at infinitely high frequency, the magnitude of the multiphoton fluorescence contribution at zero frequency, and a fluorescence lifetime; this latter quantity can be compared with the corresponding fluorescence lifetime obtained from time-correlated single-photon counting (TCSPC) experiments.

Given that extensive NMR spectral data indicate that **porphyrins 7−12** form closed-ring dimeric structures in noncoordinating solvents driven by arylamino group axial coordination to Zn (see Supporting Information), HRS measurements were carried out in THF. For HRS measurements at an 800 nm incident irradiation wavelength (λ_{inc}), experimental evidence shows clearly that no multiphoton fluorescence is present at the second harmonic wavelength of 400 nm. In contrast, the corresponding HRS measurements carried out at $\lambda_{inc} = 1300$ nm clearly show a multiphoton fluorescence contribution with growing phase delay and diminishing amplitude for increasing AM frequencies. This disparity between data collected at these two incident irradiation frequencies is surprising, given that previous studies have shown that $S_2 \rightarrow S_1$ internal conversion times are ~1 ps for monomeric (porphinato)zinc(II) complexes;[10] hence, a multiphoton absorption at $\lambda = 400$ nm that generated a real electronically excited state would be expected to produce the low energy emitting state within the ultrafast time domain. This observation that the $\lambda_{inc} = 800$ nm HRS data exhibited no multiphoton fluorescence may indicate that energy relaxation from S_2-like states occurs preferentially to lower-lying, dark charge resonance states that manifest poor Franck−Condon overlap with the S_1-state potential energy surface. Multiphoton fluorescence demodulation of the HRS signal at

(70) Beratan, D. N. In *New Materials for Nonlinear Optics*; Hann, R. A., Bloor, D., Eds.; American Chemical Society: Washington, DC, 1991; pp 89−102.
(71) Marder, S. R.; Beratan, D. N.; Cheng, L.-T. *Science (Washington, DC)* **1991**, *252*, 103−106.
(72) Clays, K.; Persoons, A. *Phys. Rev. Lett.* **1991**, *66*, 2980−2983.
(73) Clays, K.; Persoons, A. *Rev. Sci. Instrum.* **1992**, *63*, 3285−3289.
(74) Noordman, O. F. J.; van Hulst, N. F. v. *Chem. Phys. Lett.* **1996**, *253*, 145−150.
(75) Wostyn, K.; Binnemans, K.; Clays, K.; Persoons, A. *Rev. Sci. Instrum.* **2001**, *72*, 3215−3220.

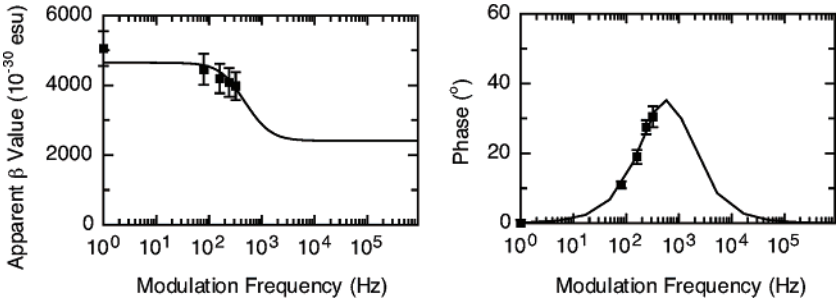

Figure 4. Typical dependence of measured β_{1300} values determined as a function of modulation frequency. Data displayed are for **porphyrin 12**; solvent = THF; $T = 293$ K.

1300 nm shows an inflection point for plots of measured β_{1300} and phase values vs modulation frequency between 100 and 300 MHz (Figure 4); simultaneous analysis of these amplitude and phase data are consistent with a fluorescence lifetime component for these compounds in the expected 1.5−0.5 ns range. The resulting dynamic hyperpolarizability values (β_{800} and β_{1300}) for these two incident irradiation frequencies are given in Table 2.

The Table 2 data highlight that extremely large dynamic hyperpolarizability values (up to 4350×10^{-30} esu) have been obtained at 1300 nm incident irradiation. Long-wavelength dynamic hyperpolarizabilities of this magnitude are a prerequisite for developing organic electrooptic modulators having increased efficiency. In this respect, note that a state-of-the-art all-organic polymeric electrooptic modulator (electrooptic coefficient r_{33} ($\lambda_{inc} = 1318$ nm) = 60 pm/V) having a half-wave drive voltage less than 1 V was based on a chromophore possessing a β_{1064} value of 3000×10^{-30} esu;[76,77] this r_{33} value rivals that of $LiNiO_3$ (32 pm/V), the solid-state inorganic reference material for nonlinear optics. It is important to appreciate that the **porphyrin 9** β_{1300} value (4350×10^{-30} esu, Table 2) is the largest yet measured at this incident irradiation wavelength for an uncharged chromophore; examples of nonlinear optical chromophores (both charged or neutral) where the measured β_{1300} value exceeds 3000×10^{-30} esu are extremely limited.[54,78,79]

Further examination of the Table 2 data shows that these superstructures exhibit complex second-order NLO properties. For example, a lower first hyperpolarizability at 1300 nm is observed for chromophores where the thiophene or oligothiophene unit is linked to the porphyrin macrocycle *meso*-carbon position via an intervening ethynyl moiety (**porphyrins 10−12**), relative to their structural analogues that feature direct connectivity (**porphyrins 7−9**) for identical numbers of thiophene units. These differences in the magnitudes of the measured first hyperpolarizabilities are explained largely by the disparate degrees of two-photon resonance enhancement at 650 nm, consistent with general expectations that derive from the classic two-level formulation of β (eq 1),[80−82]

$$\beta'_n = \frac{6(P_{ge})_n^2(\Delta\mu_{ge})_n(E_{op})_n^2}{[(E_{op})_n^2 - (2E_{inc})^2][(E_{op})_n^2 - E_{inc}^2]} \quad (1)$$

where E_{op} is the energy of the optical transition of interest, and P_{ge} and $\Delta\mu_{ge}$ are, respectively, the transition strength and ground-to-excited-state dipole moment change associated with the charge-transfer absorption. For $\lambda_{inc} = 1300$ nm, the largest resonance enhancement derives from the proximity of the Q-band transition to 650 nm. To first order, the resonance enhancement originating from the B-state manifold centered near 450 nm can be considered near constant for **porphyrins 7−12**. When we then consider only the enhancement due to Q-band proximity to $2E_{inc}$, it is clearly larger for **porphyrins 7−9** (Q-state $\lambda_{max} \approx 641$ nm) than for **porphyrins 10−12** (Q-state $\lambda_{max} \approx 684$ nm); this explains why the dynamic nonlinear response at 1300 nm for **porphyrins 7−9** is larger than that for **porphyrins 10−12**. Likewise, disparate B- and Q-state resonant enhancement effects account for the observation that the hyperpolarizability values determined at $\lambda_{inc} = 1300$ nm are larger than those measured for $\lambda_{inc} = 800$ nm for **porphyrins 7−9**.

As multiple linear optical transitions in these chromophores possess charge-transfer character,[11,12,54,83] a quantitative understanding of the frequency dispersion effects of the nonlinear optical responses require that state-specific hyperpolarizability contributions be taken into account:[84] The magnitude of these contributions to the static hyperpolarizability will be determined by the oscillator strength of the specific transition (B- and Q-state derived), the magnitude of $\Delta\mu_{ge}$, the sign of $\Delta\mu_{ge}$ (determined by the direction of the change in dipole moment between ground and excited state),[54,83,84] the magnitude of the resonance enhancement factor, and the sign of the resonance enhancement (which also effects the sign of β and depends on the position of absorption maxima relative to the fundamental and second-harmonic wavelengths). As HRS experiments only reveal the absolute magnitude of the hyperpolarizability, assumptions on state-specific dipole moment changes need to be inferred independently, similar to analyses of electroabsorption data obtained for related hyperpolarizable chromophores.[83] Further, it has long been recognized that the simple two-level model[80−82] is inadequate when an absorption band approaches either the second-harmonic or fundamental incident irradiation wavelengths, as damping effects[80] are not adequately accounted.

(76) Shi, Y.; Zhang, C.; Zhang, H.; Bechtel, J. H.; Dalton, L. R.; Robinson, B. H.; Steier, W. H. *Science (Washington, DC)* **2000**, *288*, 119.
(77) Dalton, L. R.; Steier, W. H.; Robinson, B. H.; Zhang, C.; Ren, A.; Garner, S.; Chen, A.; Londergan, T.; Irwin, L.; Carlson, B.; Fifield, L.; Phelan, G.; Kincaid, C.; Amend, J.; Jen, A. *J. Mater. Chem.* **1999**, *9*, 1905.
(78) Clays, K.; Coe, B. *Chem. Mater.* **2003**, *15*, 642−648.
(79) Tripathy, K.; Moreno, J. P.; Kuzyk, M. G.; Coe, B. J.; Clays, K.; Kelley, A. M. *J. Chem. Phys.* **2004**, *121*, 7932−7945.
(80) Oudar, J. L.; Chemla, D. S. *J. Chem. Phys.* **1977**, *66*, 2664−2668.
(81) Oudar, J. L. *J. Chem. Phys.* **1977**, *67*, 446−457.
(82) Willetts, A.; Rice, J. E.; Burland, D. M.; Shelton, D. P. *J. Chem. Phys.* **1992**, *97*, 7590−7599.
(83) Karki, L.; Vance, F. W.; Hupp, J. T.; LeCours, S. M.; Therien, M. J. *J. Am. Chem. Soc.* **1998**, *120*, 2606−2611.
(84) Moylan, C. R.; Ermer, S.; Lovejoy, S. M.; McComb, I. H.; Leung, D. S.; Wortmann, R.; Krdmer, P.; Twieg, R. J. *J. Am. Chem. Soc.* **1996**, *118*, 12950−12955.

One approach to refine the two-level model considers the impact of vibrational substates of electronic ground and excited states.[85−87] Other attempts to more correctly describe the dispersion of the first hyperpolarizability take the damping and the resulting imaginary part of the hyperpolarizability into account.[85−90] None of these approaches has been shown to accurately predict the experimental dispersion effects of a simple charge-transfer chromophore having a single CT absorption band, let alone for chromophores featuring multiple CT bands involving strongly coupled oscillators, as in the systems studied here.

The second type of structural variation within these two series of chromophores is reflected in the number of thiophene rings that separate the porphyrin macrocycle and the nitro group. Enhanced hyperpolarizabilities in classic NLO push−pull chromophore structures based on aryl donor, bridge, and acceptor components are often observed upon heteroaromatic replacement of these units, as such species possess typically a lower aromatic stabilization (delocalization) energy;[13−19,91,92] this insight has driven the synthesis of a wide range of push−pull oligothiophenyl-based second-order NLO chromophores. In accordance with well-established structure−property relationships, these chromophores show a decrease in the $S_0 \rightarrow S_1$ transition energy and an increase in first hyperpolarizability with increasing conjugation length.[91] This effect is commonly referred to in the NLO field as the nonlinearity/transparency tradeoff.[25,93]

For these structures, it is important to appreciate that oscillator strengths and frequencies of the key low energy electronic manifolds within a given chromophore series (e.g., **porphyrins 7−9**; **porphyrins 10−12**) are virtually identical (Table 2; Experimental Section; Supporting Information). For both the **porphyrin 7−9** and **porphyrin 10−12** series, the smallest hyperpolarizability values are observed for chromophores possessing only a single thiophene unit (**porphyrins 7** and **10**), while the largest NLO responses are observed when three thiophene units are incorporated (**porphyrins 9** and **12**). While any trend in these data is likely masked by strong resonance effects, a key finding of these experiments is that at $\lambda_{inc} = 1300$ nm, for chromophores that incorporate either 5-nitro-thiophene, 5-nitro-[2,2′]bithiophene, or 5-nitro-[2,2′;5′,2″]terthiophene units for a specific linkage motif to the porphyrin *meso* position, the magnitude of the measured β_{1300} value can vary substantially (Table 2). These results show that molecular structures more complex than simple uniaxial donor−acceptor charge-transfer designs can be used to circumvent the nonlinearity-transparency tradeoff. While ascertaining the precise origin of this effect will undoubtedly require additional experiments, it likely derives from the transfer of oscillator strength between overlapping $\pi-\pi^*$ and CT transitions as a function of conjugation length in these structures. In such a case, P_{ge} and $\Delta\mu_{ge}$ would effectively increase with increasing conjugation in the **porphyrin 7−9** and **porphyrin 10−12** series, thereby effecting an increase in the magnitude of the observed β_λ value while causing apparently minor perturbations to the benchmark optical spectrum for these two classes of porphyrin-based hyperpolarizable chromophores.

Along these lines, it is worth noting that octopolar molecular symmetry, and especially the supramolecular octopolar ordering of individual octopoles, has been exploited as a potential means to engineer larger second-order nonlinearities without shifting significantly the chromophore absorption manifold to the red.[94,95] While such an approach is promising, obtaining macroscopic bulk ordering of octopolar chromophores via supramolecular approaches remains challenging. In contrast, **porphyrins 7−12** show that it is also possible to increase hyperpolarizabilities in dipolar structures without substantial transition energy attenuation. The retention of a chromophoric dipole in **porphyrins 7−12** in combination with improved nonlinearities without the disadvantages of an absorption red shift is important in this regard. A permanent dipole allows electric-field poling of the individual chromophores within a bulk structure; in contrast, for apolar, octopolar chromophores, only supramolecular self-ordering, or the optical poling, is possible. Finally, it is important to note the absolute β_{1300} value ($(4350 \pm 200) \times 10^{-30}$ esu) that is obtained for the optimal structure, **porphyrin 9**, is one of the largest yet reported[54] and the greatest yet measured at $\lambda_{inc} = 1300$ nm for an uncharged chromophore.

Summary and Conclusions

An extensive series of conjugated (porphinato)zinc(II)-based chromophores featuring nitrothiophenyl and nitrooligothiophenyl electron-accepting moieties has been synthesized using metal-catalyzed cross-coupling reactions involving 5-bromo-15-triisopropylsilylethynyl-10,20-diarylporphinato]zinc(II) and an electron-rich Suzuki-porphyrin synthon, [5-(4-dimethylaminophenylethynyl)-15-(4′,4′,5′,5′-tetramethyl[1′,3′,2′]dioxaborolan-2′-yl)-10,20-diarylporphinato]zinc(II), with appropriately functionalized aryl and thienyl precursors. These donor−acceptor chromophores feature thiophenyl, [2,2′]bithiophenyl, and [2,2′;5′,2″]terthiophenyl units terminated with a 5-nitro group; one series of structures features these acceptor moieties appended directly to the porphyrin macrocycle *meso*-carbon position, while a second set utilizes an intervening *meso*-ethynyl moiety to control porphyrin-to-thienyl conjugation. The dynamic hyperpolarizabilities of these compounds were determined from hyper-Rayleigh light scattering (HRS) measurements carried out at fundamental incident irradiation wavelengths (λ_{inc}) of 800 and 1300 nm. The combined linear and nonlinear optical properties of these compounds challenge the classical concept of the nonlinearity/transparency tradeoff in charge-transfer chromophores: the magnitude of the molecular hyperpolarizability is observed to vary substantially despite approximately uniform ground-state absorptive signatures for a given porphyrin-to-thiophene linkage topology. Given that these design features described here can give rise to substantial β_{1300} values

(85) Woodford, J. N.; Wang, C. H.; Jen, A. K. Y. *Chem. Phys.* **2001**, *271*, 137−143.
(86) Pauley, M. A.; Wang, C. H. *Rev. Sci. Instrum.* **1999**, *70*, 1277−1284.
(87) Wang, C. H. *J. Chem. Phys.* **2000**, *112*, 1917−1924.
(88) Meshulam, G.; Berkovic, G.; Kotler, Z. *Opt. Lett.* **2001**, *26*, 30−32.
(89) Meshulam, G.; Berkovic, G.; Kotler, Z. *Rev. Sci. Instrum.* **2000**, *71*, 3490−3493.
(90) Berkovic, G.; Meshulam, G.; Kotler, Z. *J. Chem. Phys.* **2000**, *112*, 3997−4003.
(91) Rao, V. P.; Jen, A. K. Y.; Wong, K. Y.; Drost, K. J. *Tetrahedron Lett.* **1993**, *34*, 1747−1750.
(92) Hsu, C.-C.; Shu, C.-F.; Huang, T.-H.; Wang, C. H.; Lin, J.-L.; Wang, Y.-K.; Zang, Y.-L. *Chem. Phys. Lett.* **1997**, *274*, 466−472.
(93) Cheng, L.-T.; Tam, W.; Stevenson, S. H.; Meredith, G. R.; Rikken, G.; Marder, S. R. *J. Phys. Chem.* **1991**, *95*, 10631−10643.
(94) Verbiest, T.; Clays, K.; Samyn, C.; Wolff, J.; Reinhoudt, D.; Persoons, A. *J. Am. Chem. Soc.* **1994**, *116*, 9320−9323.
(95) Le Bozec, H.; Bouder, T. L.; Maury, O.; Bondon, A.; Ledoux, I.; Deveau, S.; Zyss, J. *Adv. Mater.* **2001**, *13*, 1677−1681.
(96) Bauerle, P. *Adv. Mater.* **1992**, *4*, 102−107.

in neutral dipolar chromophores, these data suggest that this class of conjugated, electronically asymmetric porphyrin-thiophene chromophores may find utility for electrooptic applications at telecom-relevant wavelengths.

Acknowledgment. This work was supported by a grant from the Office of Naval Research N00014-01-1-0725, the Belgian Govt. (IUAP/5/3), the Flemish Fund for Scientific Research (G.0261.04), and the U. of Leuven (G0A/2000/03).

Supporting Information Available: Syntheses and characterization data for (porphinato)zinc(II)-based chromophores **7**−**12**, key precursor structures and chromophoric benchmarks; NMR, absorption, and emission data for thiophene-, oligothiophene-, porphyrin-based compounds; tabulated solvent-dependent spectroscopic properties. This material is available free of charge via the Internet at http://pubs.acs.org.

JA0402553